2017 IEEE International Conference on Robotics and Automation (ICRA)
Singapore, May 29 - June 3, 2017

Design and Control of an Inchworm-Inspired Soft Robot with Omega-Arching Locomotion*

Huaxia Guo, Jinhua Zhang, Tao Wang, Yuanjie Li, Jun Hong, Yue Li

Abstract—**This paper presents an inchworm inspired soft robot composed of the soft body, the front foot as well as the back foot. Compared to the traditional inchworm-type robot consisting of rigid components, the driven mode for the soft robot is more simple. The soft robot inspired by the inchworm has higher locomotion efficiency than the other bionic soft robot. The main idea of this paper is to imitate the "Ω" motion shape of biology inchworm based on a silicone square tube with strain-limiting layers. Besides, each foot of the robot made through 3D printing technology together with metal sheet can produce different friction coefficients to achieve the anchor-motion movement. Then, the robot realizes an inchworm-like locomotion under certain actuation patterns. Experimental results show that the proposed robot has excellent performance.**

I. Introduction

With the development of technology, robots made of traditional mechanical components have been unable to meet the needs of daily life. Instead, soft robot composed of soft material gain advantages over the rigid robots due to its compliant structures and secure interactions between human and machine[1]. Due to the high movement efficiency of living creature, the robot inspired by inchworms has drawn so many bionic researches' attention in the recent years.

Since the "soft robotics" became a burgeoning field of study [2], numerous bionic robots have been created. These robots can be divided into two main categories. One is the operating robot that can grab or lifting weights such as the OctArm continuum manipulator [3], the jamming gripper [4]or the flexible micro actuator robot with several holding molds [5].The other aspect primarily relates to the locomotive biomimetic robot. Inspired by animals (e.g., squid, starfish, worms), Harvard University designed the multi-gait soft robot in 2011 that can demonstrate mobility by using a network of pneumatic channels [6]. In 2013, Cagdas D Onal and Daniela Rus developed the prototype of the fluidic elastomer robotic snake [7] consisting of four bidirectional fluidic elastomer actuators in series to create a traveling curvature wave from head to tail along its body. Taking caterpillars for the imitating object, Barry Trimmer et al in Tufts University designed the highly deformable 3-D printed soft robot generating inching and crawling locomotion in 2014 [8].

When devising soft robot, a combination of soft materials and stiff components is usually used in the interest of replicating the living creature's locomotion pattern. As to the motion-type bionic robot, a few studies have been conducted based on the inspiration from biological inchworm. Shohie Ueno et al researched the micro inchworm robot using electro-conjugate fluid that can move on a horizontal acrylic surface with maximum speed of 5.2mm/s [9]. Je-Sung Koh et al proposed the omega-shaped inchworm-inspired crawling robot built from a composite structure with flexural joints and SMA spring actuator [10]. Kwangmok Jung et al once developed the micro inchworm robot to provide up-down, and two rotational degree-of-free motion based on actuator modules made from non-prestrained dielectric elastomer[11]. Further robots imitating the motion of inchworm were studied under the foundation of diverse mechanical structures and actuation mechanisms [12-15].

However, all the inchworm-type robots mentioned above just involved the locomotion gait design rather than the arching peculiarity. In this study, an inchworm-inspired soft robot was proposed, manufactured and tested. Thanks to its silicone square tube with strain-limiting layers, the robot can bend and show omega shape under the driven of gaseous fluid. Besides, the front and back feet were made in order to mimic the alternating movement of the living creature. Then under certain intelligent regulation to the period as well as amplitude of air pressure, the robot can generate desired linear motion.

The rest of the paper is as follows. The description of the biological geometrid is described in Section Ⅱ, while Section Ⅲ and Ⅳ illustrate the design and fabrication of the robot components, respectively. Tests for evaluating the motion performance of the soft robot are described in Section Ⅴ. Section Ⅵ provides the conclusion of this paper.

II. Description of the Biological Inchworm

Inchworms are not worms, but caterpillars [16]. Exemplified by geometrids, the most common alternative gait is inching except for crawling. Inching has the longest possible length of step so, for a given cycle frequency, it is the fastest gait [17]. In order to excavate the prominent locomotive morphology, several tea geometrids were cultured and studied in the current study. As can be seen from fig.1 (a), the inchworm's body can stand straight when its rear foot becomes anchored. Fig.1 (b) reveals that most of the body exhibits arching during the movement. Besides, the inchworm can move up and down flexibly along the ruler, which is sketched from (c) to (f) in fig.1.

Although the inchworm has so many kinetic features, this paper focuses on the robot design in order to achieve the omega-arching shape as well as the locomotion pattern. Based on the moving characteristics of living creatures, robot designed by imitating the motion mechanism of the inchworm.

*This research is supported by the National Nature Science Foundation of China. Authors are with the State Key Laboratory for manufacturing systems Engineering, Xi'an Jiaotong University (jjshua@mail.xjtu.edu.cn).

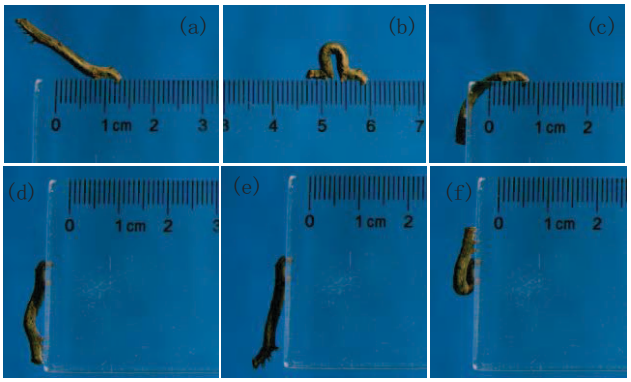

Figure.1 Diverse motility patterns of inchworm for the test use

Inchworm locomotion involves alternative releasing and grasping of the front and rear sets of legs, and arching incorporating much of the animal's length [2]. As sketched in fig.2, a single motion period of inchworm can be divided into two phases. The first phase refers to that the tail portion of the inchworm moves towards the head until most of the whole body exhibits arching, during which process the head section remains stationary. Then with the tail section becomes anchored, the rest part of the inchworm expresses the reverse performance until the arching is eliminated compared to the first phase. Once the motion of these two phases is completed, the inchworm fulfills its whole step forward.

III. Design of Inchworm-like Soft Robot

A. Structure scheme Specifications

The paper here proposes the robot structure which was compared with the bionic inchworm, seen in fig.3 (a). Be in keeping with the biological inchworm, the robot basically consists of three parts, referred to as the body, the front foot as well as the back foot. The air cavity in the body section was designed to exhibit the omega deformation when actuated. Besides, the anchor-motion mechanism was achieved on the basis of the feet set in the front and back sections of the robot respectively, as sketched in fig.3 (b). The locomotion principle of the robot depends on the anchor and motion of the feet. During the first phase of the movement process, the front foot anchors until most of the robot body exhibits arching. Then the back foot of the robot keeps fixed while the body moves forward, thus the robot accomplishes a cycle motion with a step length reflected by the front as well as the back feet

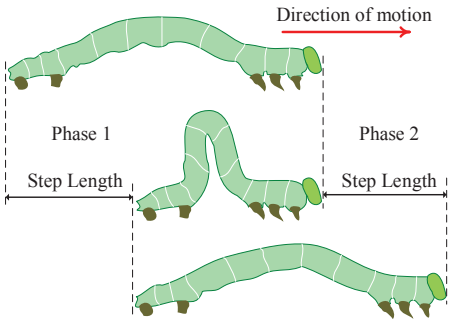

Figure.2 Schematic for a period of motion of the inchworm[18]

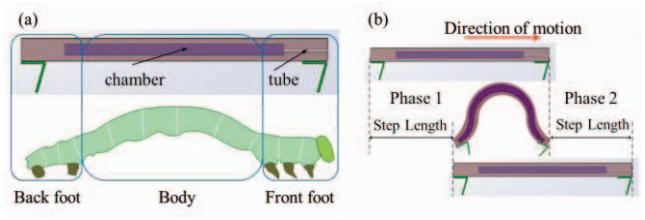

Figure.3 (a) Structure comparison between the robot structure and aninchworm. (b) Locomotive procedure for a period of motion of the robot

uniformly in theory. Determining the parameters of the structure then became the key point.

B. Body Design

Pneumatic actuation was used in the paper as the active components. The hyper-elastic material can be used if the large deformation of the robot body was wanted. However, actuators made of soft materials can only inflate into various directions, whose deformation is just like a balloon. So, materials possessing different physical attributes became the optional objects. In order to obtain the bending deformation for omega shape of the robot, a pneumatic actuator laid with the strain-limiting layers was designed. By adjusting the positions of the strain limiting layers on the soft body, the rubber tube can show the desired deformation. Meanwhile, wrapping the actuator with inextensible fibers constrains it from expanding radially. So, generally the fiber-reinforcements were needed during the design of the robot made from soft materials. The diagrammatic sketch of the robot body was illustrated in fig.4 and its specific parameters are exhibited in table 1. Keep note that the pitch for the fiber was an important parameter which can't be chosen too large and the thickness of the pneumatic actuator was selected by considering the contradiction between the cost as well as the capacity for deformation of the actuator.

The sizes raised above were all determined by means of simulation through different attempts for changing dimension parameters of the soft body. The strain limiting layer in the lower position of the soft body was used to achieve the bending of the actuator. Then the upper strain limiting layers symmetrically laid on the actuator were served to imitate the ankle shape of the inchworm. Thus the soft body can exhibit the omega shape when inflated. The software of ABAQUS was employed to forecast the shape of the soft body. As illustrated in fig.5, the deformation process of the body ranges from the original state Ⅰ to the final state 4 with one end of the tube

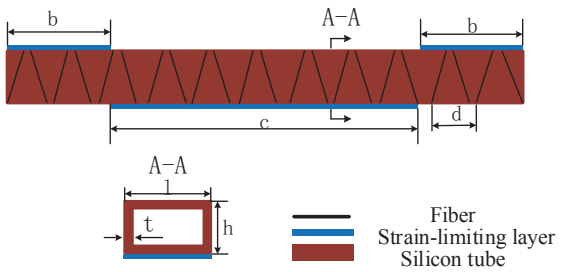

Figure.4 Schematic diagram of inchworm-like body

TABLE I BODY PARAMETERS OF THE INCHWORM ROBOT

Body parameters	Value/mm
Length of the up strain-limiting layer b	20
Length of the up strain-limiting layer c	70
Pitch for the fiber d	3
Wall thickness t	2
Sectional length l	13
Sectional height h	8

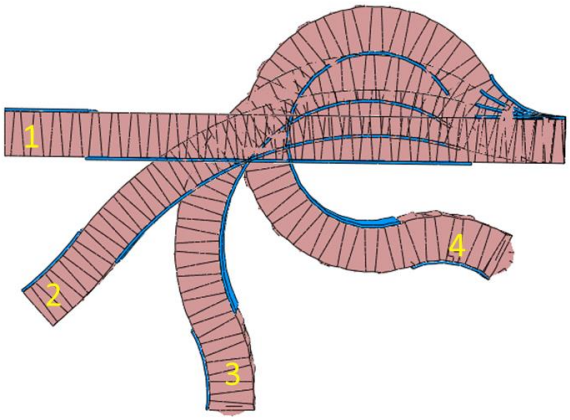

Figure.5 Simulation of the body for deformation process (left from 1 to 4) and final result (right)

fixed as the boundary restraint when inflating during simulation. And the ultimate type of the robot body shows the omega-like shape.

C. Feet Design

The feet were the important components of the inchworm-inspired robot in order to obtain the anchor-motion movement. Dongwoo Lee et al once developed the inchworm robots that can change different motion state relying on metal claws [19]. Wei wang et al also studied the inchworm-inspired robot by using the polyimide film as well as silicon segment in order to gain the relative low and high friction force with the ground [18]. Based on the same movement mechanism, this paper designed the foot with a series of angles through the 3-D printing technology. The three-dimensional sketch of the foot can be noticed in fig.6. The front as well as the back foot was with the same shape and dimension. The parameters of the foot were revealed in table Ⅱ. Then by sticking the thin metal sheet

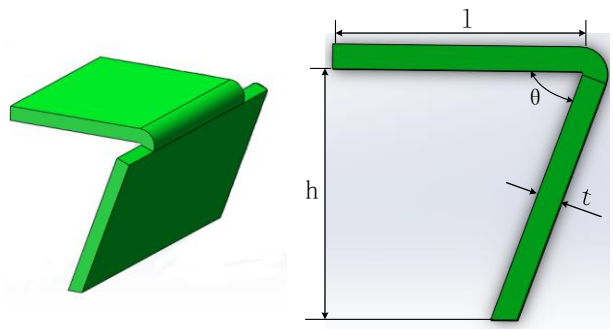

Figure.6 From left to right, three-dimensional sketch of the foot structure and its main dimension parameters

TABLE II FOOT PARAMETERS OF THE INCHWORM ROBOT

Foot parameters	Value
Angle of the foot θ/°	30,35,……70
element thickness t/mm	1.5
Horizontal length l/mm	10
Height of the foot h/mm	10

such as the feeler leaf together with the printed component, seen in fig.7, the feet in the front and back sections can achieve the anchor-motion mechanism. It is worth noting that the optimal angle for the foot will be tested in the experimental part later.

IV. FABRICATION

The main manufacturing process of the robot was comprised of two parts: the fabrication of the soft body as well as the foot. As can be seen in fig.7 (a), the body here was created following a multistep molding process. Firstly, the liquid raw material was mixed and evacuated used to form the robot body. The material used in this paper was Elastosil M4601 to be mixed in a 9:1 ratio of Part A: Part B, by weight. The performance of the material was proposed by Panagiotis Polygerinos in 2013 [20].Then the first rubber layer was molded with the strain limiting layers placed by pouring the Elastosil to the molds printed with 3-D laser rapid prototyping technique. The cavity in the body was made with the help of the core-mold.

In order to complete the whole manufacturing process of the robot body, a multiple molding approach was used. It's remarkable that the fiber-reinforcements should be added before the second pouring of the liquid thus limiting the radial expansion and promoting linear extension. When finishing the above procedures, both ends of the actuator should be covered and the air tube should be inserted into one end of the body.

The front and back feet of the robot were developed also through 3-D printing technology. Based on the three dimensional image of the robot foot seen in fig.6, the foot was produced with different angles. Then by sticking together with the silicone sealant, the feet were mounted to the soft body, thus producing the prototype of the robot seen in fig.7 (b).

V. EXPERIMENTAL ASSESSMENT OF INCHWORM ROBOT

A. Electronic and Pneumatic System

In fig.8 (a) an electronic and pneumatic control system used for experimental study of the inchworm-like robot was developed. Generally, the pressure can be regulated with the analog output (voltage) by the proportional valve (SMC/ITV0050-3ML).The solenoid valve (SMC/VT307-5H1-02) controls in-flow and out-flow of the pressure to the actuator. The entire control system was implemented under the Programmable logic controller (OMRON) that can generate PWM signals to valves. According to the user's demands, the frequency and duty cycle can be varied. A compressor was used as the gas source.

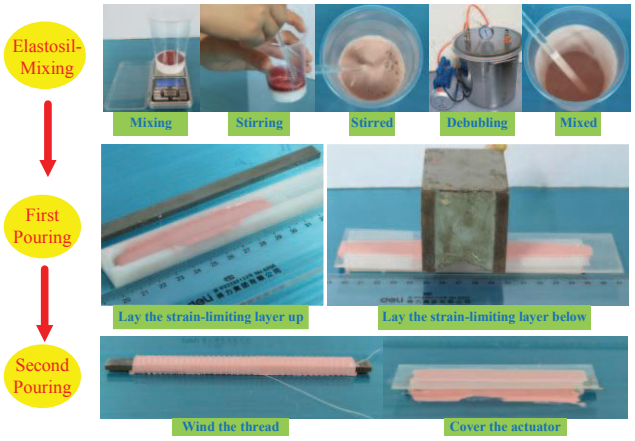

(a)

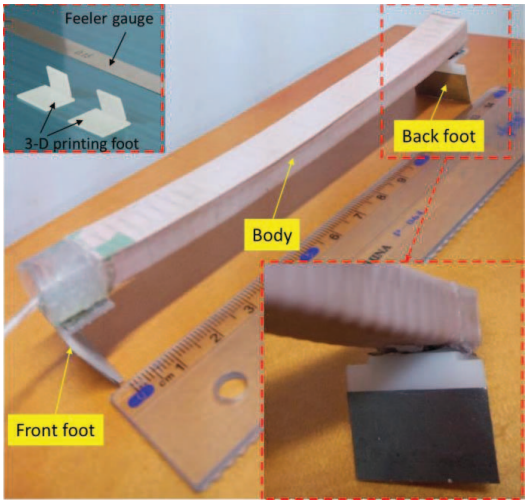

(b)

Figure.7 (a) Schematic outlining some stages of the inchworm-type robot fabrication process. (b) Inchworm-type robot prototype and its raw materials for foot

B. *Optimal Pressure selection*

For characterizing the bending performance of the actuator, the fluidic chamber was actuated. However, the bending state has much to do with the value of the air pressure. When

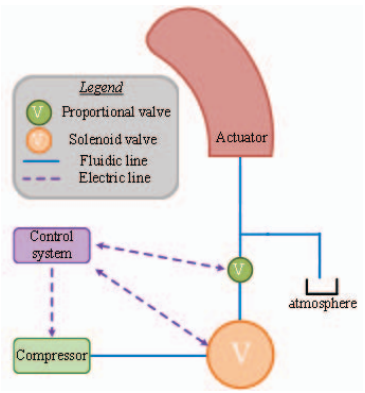

(a)

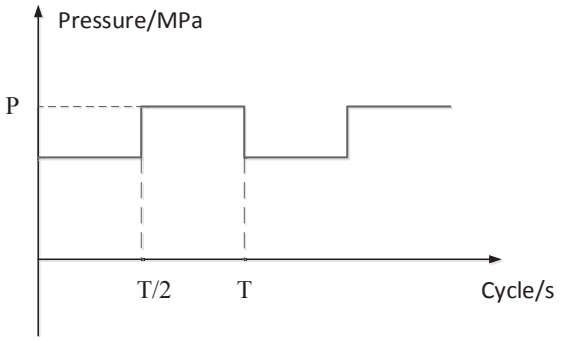

(b)

Figure.8 (a) Diagram of the pneumatic control system (b) Diagram of the control sequence for the robot produced by the control system

conducting the experiment to attain the perfect deformation for the soft body of the robot, the air pressure was increased gradually from zero with the front feet of the robot anchored. The relationship between pressure and the distance calculated between the front and the back feet of the robot was acquired. As illustrated in fig.9, we can see the distance decreases while the pressure increases. Thus according to the nearest distance between point A and B marked at the back and front feet of the soft robot, the best pressure for the deformation of the robot body was 0.3MPa. Namely, the shape of the actuator was a good approximation to omega under that value of pressure. Besides, a proper value of pressure was necessary for the optimal motion efficiency of the robot. However, it is worth noting that the value of pressure was set 0.25MPa during the experimental stage for fear of invalidity of the actuator.

The perfect angle of the robot feet was obtained under the experimental condition operated as the circumstance referred in fig.9. The experiments were conducted based on certain

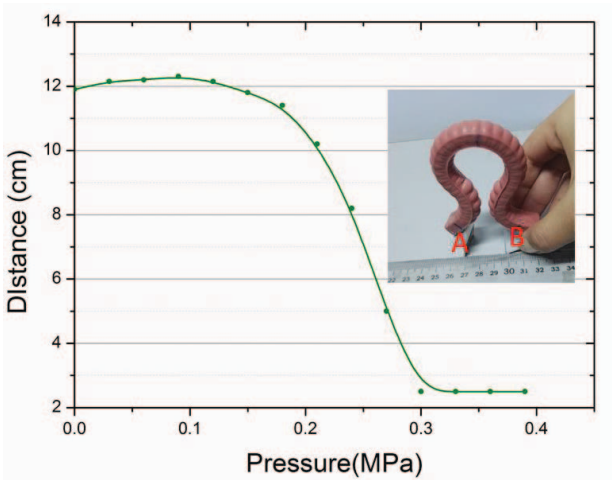

Figure.9 Relationship between pressure and the distance of robot feet

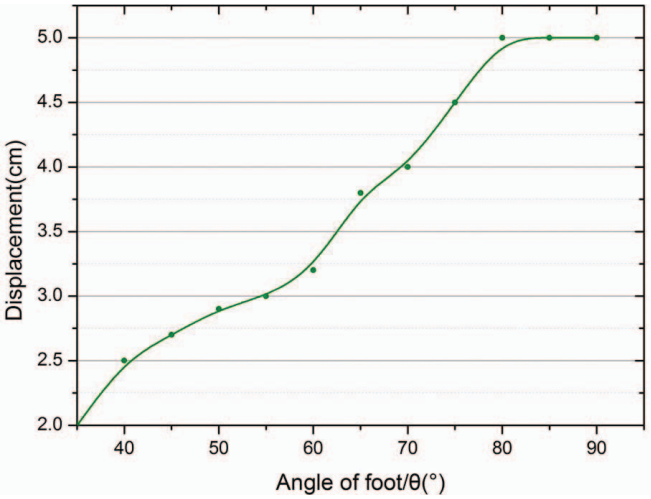

Figure.10 Relationship between the angle and displacement of the robot

inflation sequence. As can be seen in fig.8 (b), the sequential control algorithm was illustrated, where T reflects the cycle of the pressure and P represents the target pressure value for the robot chamber. On the premise of the definite values of pressure and the period, the 3-D printing feet with different angles stuck by the feeler leaf were mounted to the front and back sections of each robot and corresponding displacement were measured. The relationship between the angle of feet and the placement of robot was summarized. Result shows that adding the angle of the foot significantly increasing the displacement of the robot, drawn in figure 10, so the 80-degreee was chosen as the final angle of the robot feet to achieve the optimum movement efficiency of the robot.

C. Experimental verification

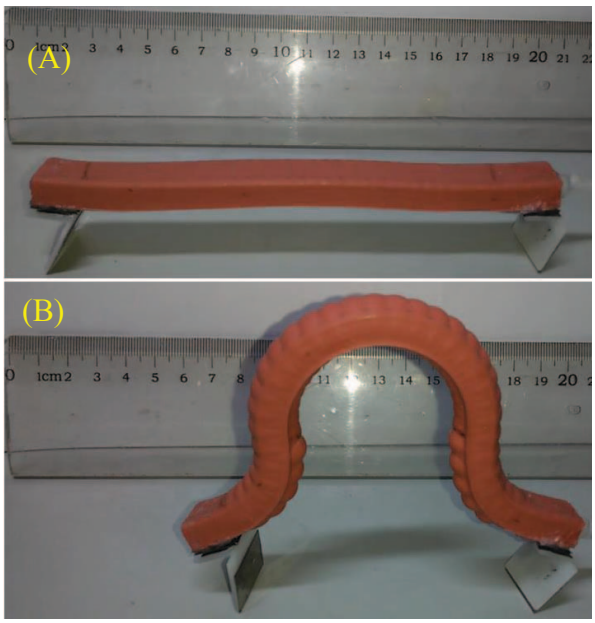

(a)

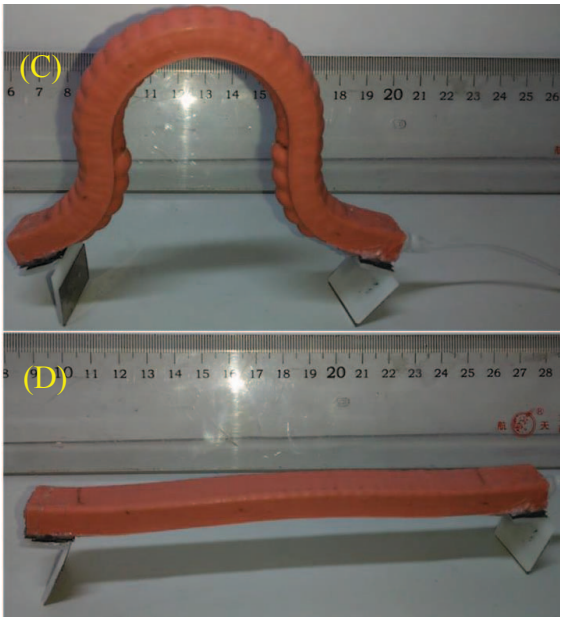

(b)

Figure.11 (a) Motion sequence for the inchworm-type robot when T=2s with (a)、(b) the first and second stage of the robot motion

the motion gait can be seen in fig.11, the soft robot realized the motion-anchor locomotion mechanism and the omega-arching shape. Fig.11 (a) illustrates the first phase of the

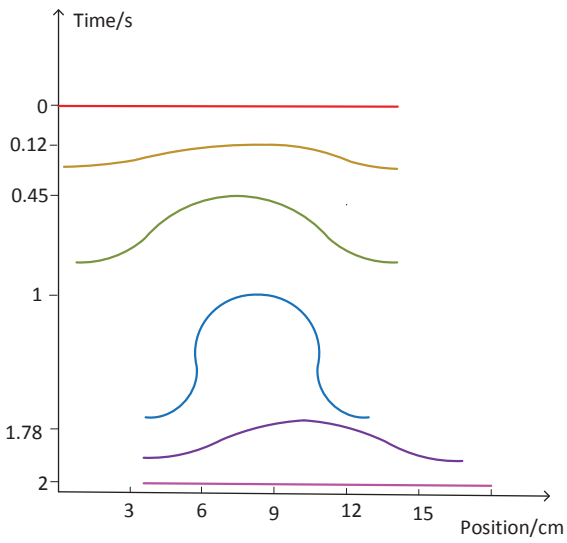

Figure.12 Curvature lines extracted during movement process for T=2s

inchworm-like robot motion. The original state of the robot can be seen in picture （A）. When the robot was actuated, most of the body part demonstrated arching with the front foot anchored which was exhibited in fig.11 (B). Picture (C) has the same state with (B). Then in the second locomotion stage of the body started stretching with the back foot keeps stationary under the condition that the air supply was cut off， as sketched in fig.11(b). In (D) we can see the soft robot returned to its original state. During the whole motion process, the feet may slide backward, but it won't affect the total efficiency of the soft robot, as reflected in the multimedia attached. So the step length in each stage was regarded as the same. The response

time of the inflating and the deflating for the soft robot was measured to be 0.5 seconds as well as 1.5 seconds respectively. The time divergence between the two changes of state was due to the hysteresis phenomenon concerning the soft material.

Based on the above analysis for the selection of parameters influencing the movement of the robot, adjusting the period of

TABLE III MOTION SPEED OF THE INCHWORM ROBOT

Period/T	Centroid Displacement (cm)	Average velocity(cm/min)
1.0	2.0	120
2.0	8.0	240
3.0	8.0	160
4.0	8.5	127.5
5.0	9.0	108
6.0	9.0	90

gas-supplying produces different speed of the soft robot. Table Ⅲ reveals the locomotion efficiency of the soft robot in which the displacement of sliding backward was considered. Result shows that the bigger of the gait cycle, the faster of the robot speed when T was larger than 2 seconds. It was mainly because that it needs enough time for the body part to resume to its original form thus the minor pressure cycle was insufficient for the robot to go through the whole locomotion process. So the data in the first line of table Ⅲ were unscientific compared to other data. The robot was able to move at the fastest speed of 240 cm/min when T was 2s, which was much faster than the largest speed of multi-gait robot with 92m/h [5].

Fig.12 exhibits the curvature lines extracted from the robot body during certain motion times which also indicating the fulfillment of both the anchor-motion mechanism as well as the omega-like shape for the inchworm-like robot. The curves in the graph correspond to the experimental situation that the values for the pressure and period were 0.25MPa as well as 2seconds respectively.

VI. CONCLUSION

In this paper the inchworm-like robot has been proposed, developed, and tested. Based on the bionic requirements, the robot consists of the body as well as the feet. Thanks to the different friction coefficients of the feet, the anchor-motion mechanism can be achieved. Besides, the robot exhibits omega shape under the action of the pneumatic actuator laid with strain-limiting layers. Experimental result indicates that the robot can achieve the biomimetic design of the inchworm involving both the arching morphology and the locomotion mechanism with a perfect motion speed. Future work will focus on improving the freedom of motion and on studying the blocking technology to achieve the variable rigidity characteristic of the robot.

ACKNOWLEDGMENT

The research work is supported by a grant from the National Nature Science Foundation of China (No.51675413).

REFERENCES

[1] N. Cheney, J. Bongard, and H. Lipson, "Evolving Soft Robots in Tight Spaces." pp. 935-942.

[2] R. H. Plaut, “Mathematical model of inchworm locomotion,” International Journal of Non-Linear Mechanics, vol. 76, pp. 56-63, 2015.

[3] W. McMahan, V. Chitrakaran, M. Csencsits, D. Dawson, I. D. Walker, B. A. Jones, M. Pritts, D. Dienno, M. Grissom, and C. D. Rahn, "Field trials and testing of the OctArm continuum manipulator." pp. 2336-2341.

[4] J. R. Amend, E. Brown, N. Rodenberg, H. M. Jaeger, and H. Lipson, “A positive pressure universal gripper based on the jamming of granular material,” IEEE Transactions on Robotics, vol. 28, no. 2, pp. 341-350, 2012.

[5] K. Suzumori, S. Iikura, and H. Tanaka, “Applying a flexible microactuator to robotic mechanisms,” IEEE control systems, vol. 12, no. 1, pp. 21-27, 1992.

[6] R. F. Shepherd, F. Ilievski, W. Choi, S. A. Morin, A. A. Stokes, A. D. Mazzeo, X. Chen, M. Wang, and G. M. Whitesides, “Multigait soft robot,” Proceedings of the National Academy of Sciences, vol. 108, no. 51, pp. 20400-20403, 2011.

[7] C. D. Onal, and D. Rus, “Autonomous undulatory serpentine locomotion utilizing body dynamics of a fluidic soft robot,” Bioinspiration & biomimetics, vol. 8, no. 2, pp. 026003, 2013.

[8] T. Umedachi, and B. A. Trimmer, "Design of a 3D-printed soft robot with posture and steering control." pp. 2874-2879.

[9] S. Ueno, K. Takemura, S. Yokota, and K. Edamura, “Micro inchworm robot using electro-conjugate fluid,” Sensors and Actuators A: Physical, vol. 216, pp. 36-42, 2014.

[10] J.-S. Koh, and K.-J. Cho, “Omega-shaped inchworm-inspired crawling robot with large-index-and-pitch (LIP) SMA spring actuators,” IEEE/ASME Transactions On Mechatronics, vol. 18, no. 2, pp. 419-429, 2013.

[11] K. Jung, J. Nam, and H. Choi, “Micro inchworm robot actuated by artificial muscle actuator based on nonprestrained dielectric elastomer,” Proceedings of SPIE - The International Society for Optical Engineering, vol. 5385, pp. 357-367, 2004.

[12] M.-S. Kim, W.-S. Chu, J.-H. Lee, Y.-M. Kim, and S.-H. Ahn, “Manufacturing of inchworm robot using shape memory alloy (SMA) embedded composite structure,” International journal of precision engineering and manufacturing, vol. 12, no. 3, pp. 565-568, 2011.

[13] J.-S. Koh, S.-M. An, and K.-J. Cho, "Finger-sized climbing robot using artificial proleg." pp. 610-615.

[14] H. Omori, T. Hayakawa, T. Nakamura, and T. Iwanaga, Development of mobile robots based on peristaltic crawling of an earthworm: INTECH Open Access Publisher, 2010.

[15] W. Wang, Y. Wang, K. Wang, H. Zhang, and J. Zhang, "Analysis of the kinematics of module climbing caterpillar robots." pp. 84-89.

[16] O. Orki, “A Model of Caterpillar Locomotion Based on Assur Tensegrity Structres,” TEL AVIV UNIVERSITY, 2012.

[17] B. Trimmer, and H.-t. Lin, “Bone-free: Soft mechanics for adaptive locomotion,” Integrative and comparative biology, vol. 54, no. 6, pp. 1122-1135, 2014.

[18] W. Wang, J.-Y. Lee, H. Rodrigue, S.-H. Song, W.-S. Chu, and S.-H. Ahn, “Locomotion of inchworm-inspired robot made of smart soft composite (SSC),” Bioinspiration & biomimetics, vol. 9, no. 4, pp. 046006, 2014.

[19] D. Lee, S. Kim, Y.-L. Park, and R. J. Wood, "Design of centimeter-scale inchworm robots with bidirectional claws." pp. 3197-3204.

[20] P. Polygerinos, S. Lyne, Z. Wang, L. F. Nicolini, B. Mosadegh, G. M. Whitesides, and C. J. Walsh, "Towards a soft pneumatic glove for hand rehabilitation." pp. 1512-1517.